Journal of Metals, Materials and Minerals, Vol.28 No.2 pp.115-123, 2018

Recycled poly(ethylene terephthalate)/polypropylene/wollastonite composites using PP-g-MA as compatibilizer: Mechanical, thermal and morphological properties

P. CHAIWUTTHINAN[1], S. SUWANNACHOT[2], and A. LARPKASEMSUK[2,*]

[1]*MTEC, National Science and Technology Development Agency (NSTDA), Thailand Science Park, Klong Luang, Pathum Thani, 12120, Thailand*
[2]*Department of Materials and Metallurgical Engineering, Faculty of Engineering, Rajamangala University of Technology Thanyaburi, Pathum Thani 12110, Thailand*

***Corresponding author e-mail:** amnouy.l@en.rmutt.ac.th

Received date:
7 August 2018
Revised date:
30 November 2018
Accepted date:
30 November 2018

Keywords:
Recycled PET
Polypropylene
PP-g-MA
Wollastonite
Mechanical properties
Morphology
Thermal behaviors

Abstract

Polymers investigated in this study were recycled poly(ethylene terephthalate) (rPET) as a major phase (matrix) and virgin polypropylene (PP) as a minor phase (dispersed phase). Initially, rPET was melt mixed with four different PP contents (10–40 wt%) on a co-rotating twin screw extruder and then injection molded. The blend at 30 wt% PP exhibited the highest impact strength and elongation at break and an acceptable tensile strength and Young's modulus. The 70/30 (w/w) rPET/PP blend was then upgraded its compatibility using 1–7 parts by weight per hundred of blend resin (phr) of maleic anhydride grafted PP (PP-*g*-MA). Among the compatibilized blends, that with 3 phr PP-*g*-MA imparted the highest impact strength and elongation at break owing to the better phase interaction. Therefore, the 70/30/3 (w/w/phr) rPET/PP/PP-*g*-MA compatibilized blend was selected for preparing composites with 5–20 phr of ultrafine wollastonite (WLN) in order to widen its applications. The effects of WLN content on mechanical properties (impact and tensile tests), thermal behaviors (differential scanning calorimetry and heat distortion temperature (HDT)) and morphology (scanning electron microscopy) of the composites were then investigated. The results showed that the tensile strength, Young's modulus and HDT of the composites were enhanced by up to 1.1-, 1.5- and 1.3-fold, respectively, over those of the neat compatibilized blend in a WLN-dose-dependent manner, whereas the impact strength and elongation at break only decreased slightly. This finding was due to the high aspect ratio, stiffness and thermal resistance of the WLN.

1. Introduction

It is well established that poly(ethylene terephthalate) (PET) is considered as the most important commercial polyester and one of the most important engineering polymers being widely used for many applications, especially in the textile and packaging industries [1–5]. The excessively large consumption and disposal of PET-based postconsumer products cause a major problem to the environment due to its ability to exist in the environment without significant loss of its physical properties for a long period of time [2,6–8]. Recycling of PET waste is an important issue according to the environmental impact of petroleum-based polymer production. Moreover, the quantity and quality of PET waste are high enough to support recycling investment [2]. With an efficient recycling system, discarded postconsumer PET is then sorted, collected, recovered and finally recycled into the value-added products [9,10]. Although, the mechanical and thermal properties of the recycled PET (rPET) products are deteriorated during the mechanical recycling process according to the thermomechanical and hydrolytic degradations induced by the heat, stress and moisture [2,10–13], this technique is still recommended due to its ecological and economical profits [2]. The addition of an appropriate polymer and/or reinforcing filler to the rPET is an effective method to improve certain properties with a consequential broadening of its utilization [1,2,12–16]. The melt blending of rPET with other thermoplastics has received considerable attention as a potential solution to solid waste management, among which isotactic polypropylene (PP) in particular has attracted an increasing level of commercial interest [1].

DOI: 10.14456/jmmm.2018.34

The PP is a non-polar thermoplastic polymer that belongs to the group of polyolefin and commodity plastic. It is used in a wide applications due to its high toughness, flexibility, resistance to fats and all organic solvents, low cost and easy processability [1,17–19]. These properties suggest PP is an option for blending with rPET to increase the applications of the resulting blended recycled products. Hence, the combination of rPET and PP may offer some advantages over the neat rPET. Meanwhile, the rPET can enhance the stiffness of PP at higher temperatures while the PP facilitates crystallization of rPET through heterogeneous nucleation [3,20]. A series of rPET/PP blends with increasing PP levels were then investigated. However, these blends has a problematic process due to their phase incompatibility [17,20], which limits an improvement in the thermal and mechanical properties of such blends. This drawback can be solved by adding compatibilizer or coupling agent to reduce the interfacial tension and increase the adhesion between the two phases. The most commonly used compatibilizer for PET/PP blend is PP-based polymer, such as maleic anhydride grafted PP (PP-*g*-MA) and glycidyl-methacrylate grafted PP [3,17]. In this study, the rPET/PP blend with optimum impact strength and elongation at break was filled with different amount of PP-*g*-MA (1–7 parts by weight per hundred of rPET/PP blend, phr), to try to improve their interfacial adhesion. The effects of PP-*g*-MA were then examined with fourier transform infrared spectroscopy (FTIR), mechanical analysis, and scanning electron microscopy (SEM). Thereafter, the compatibilized rPET/PP blend with the highest impact strength and elongation at break was further upgraded by adding with wollastonite (WLN), an inorganic reinforcing filler, which is a calcium metasilicate ($CaSiO_3$) mineral that occurs naturally in an acicular (needle-shaped) crystal structure with a high aspect ratio (L/D of 10-20) as shown in Figure 1 (magnification of 500×). It is theoretically comprised of 48.25 wt% CaO and 51.75 wt% SiO_2 [2,18,20–22]. The WLN used in the polymer industries has a high chemical purity with a range of desirable properties including a high chemical and thermal stability, low coefficient of thermal expansion and water absorption, high level of whiteness and hardness (Moh's hardness 4.8), small health hazard compared to asbestos, and a very low cost [2,18,20–22]. In this study, the ultrafine WLN (2000 mesh) was added at various loading levels (5–20 phr) to the rPET/PP blend to produce composite materials with improved mechanical properties as well as thermal stability and performance. The influences of the WLN were subsequently studied with mechanical analysis, scanning electron microscopy (SEM), differential scanning calorometry (DSC) and heat distortion temperature (HDT).

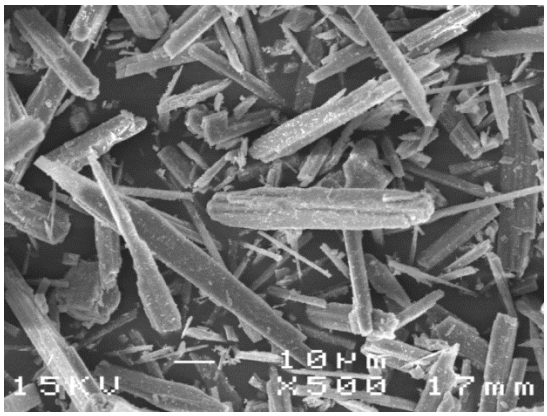

Figure 1. Representative SEM image of the ultrafine wollastonite (×1,500).

2. Experimental

2.1 Materials

The rPET flakes were mainly obtained from scrap of postconsumer bottles. Commercial PP (1100 NK) with a melt flow index of 11 g·10 min^{-1} (230°C/2.16 kg) and a processing temperature in the range 190–240°C, was obtained from IRPC Public Company Limited (Thailand). PP-*g*-MA (Bondyram 1001) with a percent grafting at 1.2 was supplied from Polyram Plastic Industries (Israel). WLN (HJ-2000) with a density and particle size of 2.85 g·cm^{-3} and 5–10 μm, respectively was supplied by H&J Mineral Fiber Technology Co. (China). All ingredients were used as received.

2.2 Preparation of polymer blends and composites

Firstly, the rPET and PP were dry mixed at four different weight ratios (90/10, 80/20, 70/30 and 60/40 rPET/PP) in a mixer (Bosco Engineering Co., Ltd., Thailand) for 10 min and then oven dried at 80°C for 12 h to remove any trace of moisture before melt blended on a co-rotating twin-screw extruder (CTE-D16L512, Chareon TUT Co., Ltd., Thailand) with a 15.75 mm screw diameter and 32 L/D ratio, operated at 240–275°C from the feed zone to the die with a screw speed of 50 rpm. The extrudates were subsequently pelletized, dried at

80°C for 12 h, and then fabricated into the standard impact and tensile test specimens using an injection molding machine (Arburg Allrounder 470°C, Germany) operated at 245°C. The blend with optimum impact strength and elongation at break was further chosen for improving their compatibility by filling with four loadings of PP-*g*-MA (1, 3, 5 and 7 phr). Again, the compatibilized blend with the highest impact strength and the acceptable tensile properties was then selected for preparing composites by extrusion and injection molding as above but with the addition of one of four loadings of WLN (5, 10, 15 and 20 phr).

2.3 Characterization of the samples

The chemical structures of the samples were characterized for their functional groups by Fourier transform infrared (FT-IR) spectroscopy on a Nicolet Nexus 470 FT-IR ESP Spectrometer (USA) over a frequency range of 650–4,000 cm^{-1}.

The notched Izod impact test was conducted on a test sample with dimension of 12.7 × 63.5 × 3 mm^3 using an impact tester (Ceast 9709, Italy) according to ASTM D256. The tensile test was performed on a standard dumbbell-shaped specimen according to ASTM D638 (Type I) using a universal testing machine (Hounsfield H 50 KS, UK) with a 10 kN load cell and at a crosshead speed of 50 $mm \cdot sec^{-1}$. The value of each property was obtained from the average of at least five specimens for each composition.

The morphology of WLN particles and impact fractured surface was observed by an SEM (Jeol JSM 6510, Japan) at an accelerated voltage of 15 and 20 kV, respectively. Prior to observation, gold was sputter coated on the specimens for electron conductivity.

The thermal behaviors of the samples were determined by a DSC analyzer (Netzsch DSC 200 F3, Germany) under a nitrogen atmosphere with a gas flow rate of 60 $mL \cdot min^{-1}$ throughout the experiment. The sample (about 10 mg) was heated from room temperature (RT) to 230°C (first heating scan) and held isothermally for 2 min to erase any previous thermal history of the material and then cooled down to room temperature (cooling scan). The sample was then reheated to 230°C (second heating scan) and cooled down to room temperature. All measurements were conducted at the same heating/cooling rate of $10°C \cdot min^{-1}$. The obtained thermograms provided crystallization temperature (T_c), melting temperature (T_m) and enthalpy of crystallization (ΔH_c), while the degree of crystallinity (χ_c) was calculated using the following equation:

$$\chi_c\ (\%) = [\Delta H_c / \Delta H^\circ_m w] \times 100$$

where ΔH^o_m is the heat of fusion for 100% crystalline of rPET (120 $J \cdot g^{-1}$) and PP (207 $J \cdot g^{-1}$) [1,2,19] and w is the weight fraction of each component in the samples.

For the HDT test, a constant bending load of 0.455 MPa was applied at the center of a bar sample (13 × 127 × 3 mm^3) which was placed in an oil bath of the heat deflection tester (Ceast, Italy), according to ASTM D648 (Method A). The sample was heated at the rate of 2 ± 0.2°C·min^{-1} from room temperature. The HDT was achieved when the specimen deflected to a distance of 0.25 mm.

3. Results and discussion

3.1 FT-IR analysis

Figure 2 shows the FT-IR spectra of rPET, PP and the 70/30/3 (w/w/phr) rPET/PP/PP-*g*-MA blend with and without WLN. All the samples containing rPET (Figures 2(a–f)) showed the characteristic peaks of carbonyl group (C=O) in conjugation with aromatic ring at 1714 cm^{-1}, asymmetric C-C-O stretching involving the carbon in aromatic ring at 1240 cm^{-1}, O-C-C asymmetric stretching at 1092 cm^{-1}, aromatic C-H wagging at 722 cm^{-1}, C-H stretching at 2950, 2918 and 2836 cm^{-1}, CH_2 deformation at 1450 cm^{-1} and symmetric CH_3 deformation at 1375 cm^{-1}, while the samples containing PP (Figures 2(b–g)) also showed the characteristic peaks of C-H stretching at 2950, 2918 and 2836 cm^{-1}, CH_2 deformation at 1450 cm^{-1} and symmetric CH_3 deformation at 1375 cm^{-1}. However, the peak intensity of the ester group (1714 cm^{-1}), asymmetric C-C-O stretching (1240 cm^{-1}), O-C-C asymmetric stretching (1092 cm^{-1}) and aromatic C-H wagging (722 cm^{-1}) in the 70/30 (w/w) rPET/PP blend [23–25] and its composites were found to be decreased by the addition of PP-*g*-MA, suggesting that maleic anhydride groups were used up or reacted with the –OH or –COOH end groups of rPET in the blend and composites during the melt mixing according to the anhydride ring opening mechanism. Therefore, the miscibility of the two incompatible polymers would be enhanced.

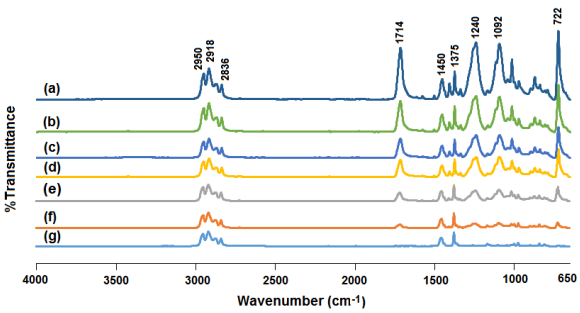

Figure 2. FT-IR spectra of (a) rPET, (b) 70/30/3 rPET/PP/PP-*g*-MA blend and (c–f) 70/30/3 rPET/PP/PP-*g*-MA composites with 5, 10, 15 and 20 phr WLN, respectively, and (g) PP.

3.2 Mechanical properties

The notched impact strength and tensile properties (elongation at break, tensile strength and Young's modulus) of the investigated samples are all summarized in Table 1. It is seen that the rPET exhibited as a brittle and stiff polymer, owing to its very low impact strength (8.6 J·m^{-1}) and elongation at break (3.2%) and rather high Young's modulus (1576 MPa), while the PP showed a kind of tough polymer due to its much higher impact strength (27.8 J·m^{-1}) and elongation at break (9%) and also lower Young's modulus (1306 MPa). With this respect, the toughness of the rPET would be improved by the addition of an appropriate amount of the PP. In this work, the rPET was melt mixed with 10–40 wt% of the PP. Among the four rPET/PP blends, the blend at 30 wt% PP exhibited the highest impact strength (23.2 J·m^{-1}) and elongation at break (5.2%), as a consequence of the superior dispersion of the PP in the rPET matrix. The impact strength and elongation at break of the blend at 30 wt% PP increased 2.7- and 1.6-fold, respectively over those of the rPET, indicating that the blend shifted from the brittleness of rPET to being tougher. However, the impact strength and elongation at break of the blend did not further increase at higher PP loading (40 wt%), owing to an aggregation of the excess PP, and thus limited the increase in the toughness of the blend. Additionally,

Table 1. Mechanical properties of the samples.

Sample	Impact strength (J·m^{-1})	Elongation at break (%)	Tensile strength (MPa)	Young's modulus (MPa)
rPET	8.6 ± 2	3.2 ± 0.7	45.4 ± 4.6	1576 ± 37
iPP	27.8 ± 4.6	9 ± 0.3	33.4 ± 0.5	1306 ± 100
rPET/PP (w/w)				
90/10	16.7 ± 2	3.9 ± 2.1	35.7 ± 13.4	1491 ± 63
80/20	18.7 ± 3.5	3.4 ± 1.2	34.4 ± 5.5	1433 ± 70
70/30	23.2 ± 5.7	5.2 ± 1.5	35.3 ± 3.5	1439 ± 58
60/40	10.7 ± 1.4	2.9 ± 0.6	26 ± 3	1331 ± 29
rPET/PP/PP-g-MA (w/w/phr)				
70/30/1	15.9 ± 0.2	6.4 ± 0.8	49.6 ± 2	1813 ± 234
70/30/3	25.4 ± 0.2	7.2 ± 0.7	46.3 ± 2.2	1818 ± 210
70/30/5	21.2 ± 0.2	6.2 ± 0.3	50.9 ± 1.8	1886 ± 150
70/30/7	23.3 ± 0.2	4.2 ± 0.4	43.1 ± 1.2	1881 ± 149
rPET/PP/PP-g-MA/WLN (w/w/phr/phr)				
70/30/3/5	20.5 ± 0.3	4.5 ± 0.9	50.1 ± 5.9	2223 ± 45
70/30/3/10	22.6 ± 0.2	4.6 ± 0.8	50.3 ± 3.8	2600 ± 72
70/30/3/15	24.5 ± 0.2	4.7 ± 0.5	49.0 ± 1.5	2660 ± 82
70/30/3/20	23.7 ± 0.2	3.8 ± 0.6	48.3 ± 2.4	2721 ± 112

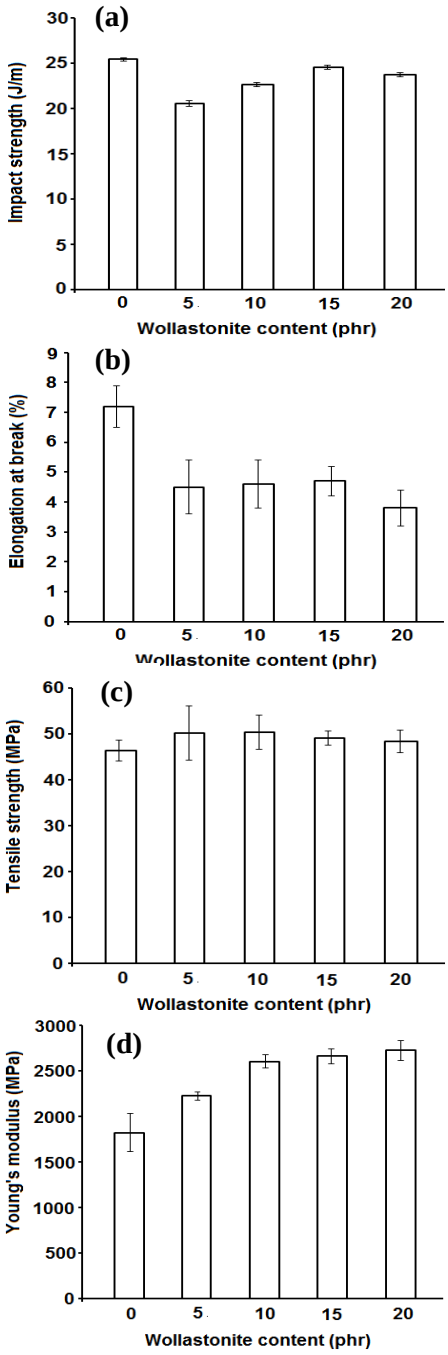

Figure 3. Mechanical properties of the composites as a function of the WLN content in terms of (a) impact strength, (2) elongation at break, (c) tensile strength and (d) Young's modulus.

the inclusion of the PP caused a dose-dependent decrease in the tensile strength and Young's modulus of the blends, according to the low tensile strength (33.4 MPa) and Young's modulus of the PP compared to those of the rPET (46.4 MPa for tensile strength). Thereafter, different weight percentages of the PP-*g*-MA (1, 3, 5 and 7 phr) was further used as a compatibilizer in the 70/30 (w/w) rPET/PP blend. Among the three compatibilized blends, the one with 3 phr PP-*g*-MA exihibited the highest impact strength and elongation at break with an accepatable tensile strength and Young's modulus. This may be due to the better compatibilizing efficiency for the rPET/PP blend that enhanced the phase interaction and the stress transfer across the two polymers. Again, the 70/30/3 (w/w/phr) rPET/ PP/PP-*g*-MA blend was then chosen for preparing composites with four loading levels of the ultrafine WLN (5, 10, 15 and 20 phr). The mechanical properties of all the composite samples compared with those of the neat rPET, PP and compatibilized blend are presented in Table 1 and also showed in Figure 3. It is evident that all the composites exhibited a decrease in the impact strength (Figure 3(a)) and elongation at break (Figure 3(b)), along with an increase in the tensile strength (Figure 3(c)) and Young's modulus (Figure 3(d)) compared with the neat compatibilized blend (0 phr WLN). The decrease in the impact strength and elongation at break and the increase in the Young's modulus may be mainly attributed to the inherent rigidity of WLN particles that hindered the mobility of the polymer chains and also due to the poor polymer-WLN interaction. An increase in the tensile strength of the composites over those the neat compatibilized blend may be related to the high aspect ratio and orientation ability of the anisotropic (fiber-like) WLN particles in the injection-molded samples, where the tensile stress was applied parallelly to the filler alignment. However, the mechanical properties of all the composites were higher than those of the neat rPET.

3.3 Morphology

Representative SEM images (magnification of 1,000×) of the impact fractured surface samples are shown in Figure 4. The neat rPET exhibited a relatively flat and smooth surface according to its brittle failure behavior (Figure 4(a)), while the neat PP (Figure 4(b)) and 70/30 (w/w) rPET/PP blend (Figure 4(c)) showed rougher surfaces due to its higher toughness. The blend filled with 3 phr PP-*g*-MA (Figure 4(d)) exhibited much rougher fractured surface, due to the compatibilizing efficiency for rPET/PP blend by promoting a fine dispersed phase morphology. The high level of plastic deformation of the compatibilized blend confirmed an increase in its impact strength over the uncompatibilized one as previously discussed. From Figures 4(e) –4(h), the fractured surfaces of the prepared blend

composites showed much different morphology compared to that of the neat blend. Large aggregates of the WLN were detached from the matrix during fracture, and so leaving the pulled out WLN particles and holes on their fractured surfaces, especially at high WLN content. The clear boundaries and interstices at the matrix-particle interface indicated the non-wettability of the WLN by the polymer matrices, which in turn reduced the impact strength of the composites as previously mentioned. However, the iPP minor phase remained as tiny globules within the rPET matrix, while the tip of the WLN particles could be seen due to their orientation in the flow direction of the injection-molded samples.

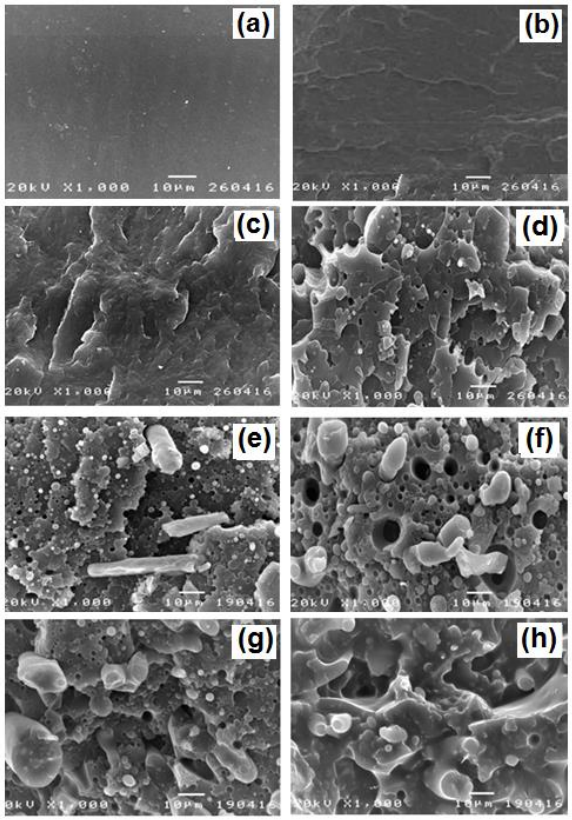

Figure 4. Representative SEM images of (a) rPET, (b) PP, (c) 70/30 rPET/PP blend (d) 70/30/3 rPET/PP/PP-*g*-MA blend, and (e–h) 70/30/3 rPET/PP/PP-*g*-MA composites with 5, 10, 15 and 20 phr WLN, respectively.

3.4 Thermal behaviors

DSC was used for studying the melting and crystallization of the samples. The DSC thermograms obtained during the cooling and second heating scans are shown in Figure 5, and the corresponding data are summarized in Table 2. Either neat rPET or PP displayed single T_c upon cooling at 194.8 and 110.2ºC, respectively. It can be seen that both polymers crystallized separately in the compatibilized blend and its composites, showing two distinct crystallization peaks. The T_c of both rPET (205.7ºC) and PP (119.9ºC) components in the compatibilized blend increased by 10.9 and 9.7ºC, respectively, suggesting that they may act as nucleating sites for the crystallization of each other [1]. However, the χ_c of rPET was reduced with the presence of the PP component. This finding may be because during cooling the rPET became solid first, while the PP is still in a molten state, and so the mobility of rPET chains was reduced, thereby acting as nucleation sites for the PP. Moreover, the PP had more time for crystallization, leading to an increased χ_c. In addition, the T_c of both rPET and PP components gradually increased with increasing WLN content in the composites, indicating the nucleating effect of WLN, especially for the PP as evidenced by its obviously enhanced χ_c. Moreover, the T_m of the neat rPET and PP was 248.8 and 160.8ºC, respectively, while that of the rPET and PP components in the compatibilized blend and composites were found to be in a narrow range of 248.7–249.9ºC and 160.8–163.5ºC, respectively. This indicated that the addition of WLN had no significant effect on the melting behavior of both rPET and PP components in the composites.

To evaluate thermal resistance, HDT was measured. The HDT results of the samples are illustrated in Figure 6. It is seen that the HDT of the neat rPET, Sample A (65°C) was much lower than that of the neat PP, Sample G (96.6°C). Hence, the HDT of the neat compatibilized blend, Sample B (70°C) was found to be increased by 1.1-fold over that of the rPET, according to the high HDT value of the added PP. In addition, the inclusion of WLN (5, 10, 15 and 20 phr) into the compatibilized blend caused an increase in the HDT of the composites from 72 to 90°C in a WLN-dose-dependent manner, owing to the high thermal resistance and stiffness of WLN particles that prevented the deformation and hindered the mobility of the polymer chains under a constant bending load during heating [26].

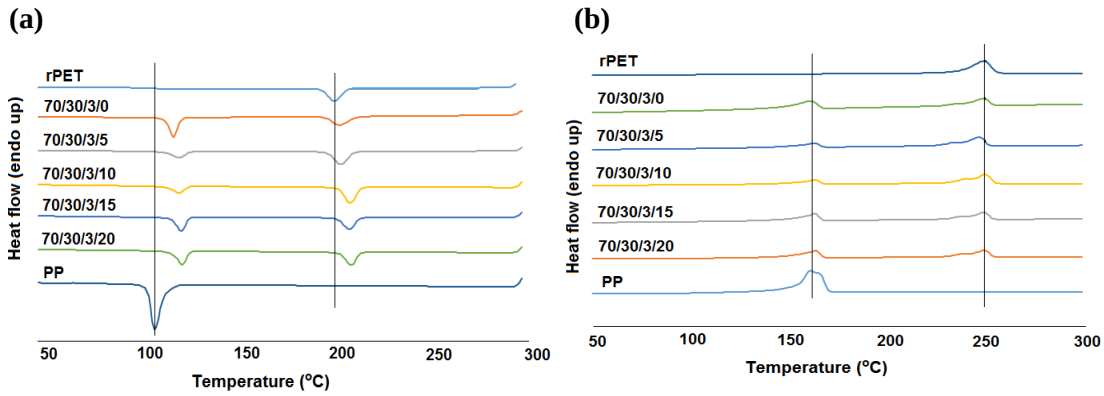

Figure 5. DSC thermograms of rPET, PP, 70/30/3 rPET/PP/PP-*g*-MA compatibilized blend and 70/30/3/x rPET/PP/PP-*g*-MA/WLN composites (where x = 5, 10, 15 and 20) obtained from (a) cooling scan, and (b) second heating scan.

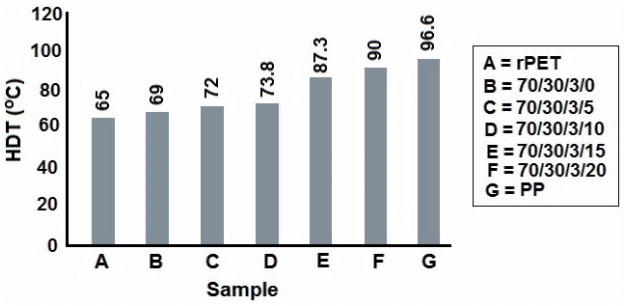

Figure 6. HDT of the samples where A = rPET, B = 70/30/3 rPET/PP/PP-*g*-MA blend and C–F = 70/30/3 rPET/PP/PP-*g*-MA composites with 5, 10, 15 and 20 phr WLN, respectively, and G = PP.

Table 2. DSC-derived data of the samples.

Sample	T_c (°C)		T_m (°C)		ΔH_c (J/g)		χ_c (%)	
	rPET	PP	rPET	PP	rPET	PP	rPET	PP
rPET	194.8	–	248.9	–	49.7	–	41.4	–
PP	–	110.2	–	160.8	–	53.9	–	25.8
rPET/PP/PP-g-MA/(w/w/phr/phr)								
70/30/3/0	205.7	119.9	248.8	160.8	19.7	29.3	24.1	44.2
70/30/3/5	206.4	121.4	248.7	163.3	9.6	41.2	12.3	64.2
70/30/3/10	209.3	122.8	249.9	163.2	9.1	41.3	12.2	68.8
70/30/3/15	210.9	123.9	249.1	163.0	15.3	29.9	21.6	51.6
70/30/3/20	211.8	124.2	249.3	163.5	16.2	31.5	23.7	56.4

4. Conclusions

Polymer blends and composites based on rPET, PP and WLN using PP-*g*-MA as compatibilizer were successfully prepared on a co-rotating twin screw extruder and injection molding machine. The effect of PP contents (10–40 wt%) on mechanical properties (impact and tensile testing) of rPET/PP blends was first investigated. The results showed that the PP played an important role as a toughening agent for the rPET. The blend at 30 wt% PP exhibited the highest impact strength and elongation at break, but at the expense of reducing the tensile strength and Young's modulus. In an attempt to improve their compatibility, this blend composition was then added with 1–7 phr PP-*g*-MA. It was found that the compatibilized blend with 3 phr PP-*g*-MA revealed the highest compatibilizing

efficiency as evidenced by its highest impact strength and elongation at break, along with an increase in the tensile strength and Young's modulus compared to those of the neat rPET and compatibilized blend. Afterwards, four loadings of the WLN (5–20 phr) were added to the compatibilized blend with 3 phr PP-*g*-MA. The incorporation of WLN was found to enhance the tensile strength, Young's modulus and HDT of the composites over those of the neat compatibilized blend with a slight decrease in the impact strength and elongation at break. However, the mechanical properties and thermal resistance of all the composites were higher than those of the rPET. Hence, it can be concluded that the use of PP, PP-*g*-MA and WLN in an appropriate amount effectively improved the properties and performance of the waste PET.

5. Acknowledgements

The authors acknowledge the Department of Materials and Metallurgical Engineering, Faculty of Engineering, Rajamangala University of Technology, MTEC, National Science and Technology Development Agency (NSTDA), Associate Professor Saowaroj Chuayjuljit and Assistant Professor Dr. Anyaporn Boonmahitthisud for financial, material and instrument support.

References

[1] M. Kuzmanović, L. Delva, L. Cardon, and K. Ragaert, "The effects of injection molding temperature on the morphology and mechanical properties of PP/PET blends and microfibrillar composites," *Polymers*, vol. 8, pp. 1–16, 2016.

[2] S. Chuayjuljit, P. Chaiwutthinan, L. Raksaksri, and A. Boonmahitthisud, "Effects of poly (butylene adipate-*co*-terephthalate) and ultrafined wollastonite on the physical properties and crystallization of recycled poly(ethylene terephthalate)," *Journal of Vinyl and Additive Technology*, vol. 23, pp. 106–116, 2015.

[3] L. M. G. Guadagnini and A. R. Morales, "Compatibilization of recycled polypropylene and recycled poly(ethylene terephthalate) blends with SEBS-g-MA," *Polimeros*, vol. 28, pp. 84–91, 2018.

[4] J. H. Lee, K. S. Lim, W. G. Hahm, and S. H. Kim, "Properties of recycled and virgin poly(ethylene terephthalate) blend fibers," *Journal of Applied Polymer Science*, vol. 128, pp. 1250–1256, 2013.

[5] I. Acar, A. kaşgőz, S. Őzgűműs, and M. Orbay, "Modification of waste poly(ethylene terephthalate) (PET) by using poly(L-lactic acid) (PLA) and hydrolytic stability," *Polymer-Plastics Technology and Engineering*, vol. 45, pp. 351–359, 2006.

[6] X. Luo and Y. Li, "Synthesis and Characterization of Polyols and Polyurethane Foams from PET Waste and Crude Glycerol," *Journal of Polymers and the Environment*, vol. 22, pp. 318-328, 2014.

[7] L. Tan, Y. Chen, W. Zhou, F. Li, L. Chen, and X. He, "Preparation and biodegradation of copolyesters based on poly(ethylene terephthalate) and poly(ethylene glycol)/oligo (lactic acid) by transesterification," *Polymer Engineering and Science*, vol. 50, pp. 76–83, 2010.

[8] S. K. Najafi, "Use of recycled plastics in wood plastic composites – A review," *Waste Management*, vol. 33, pp.188–1905, 2013.

[9] F. Awaja and D. Pavel, "Recycling of PET," *European Polymer Journal*, vol. 41, pp. 1453–1477,

[10] S. Mbarek and M. Jaziri, "Recycling poly (ethylene terephthalate) waste: properties of poly(ethylene terephthalate)/polycarbonate blends and the effect of a transesterification catalyst," *Polymer Engineering and Science*, vol. 46, pp. 1378–1386, 2006.

[11] N. Kerboua, N. Cinausero, T. Sadoun, and J. M. Lopez-Cuesta, "Effect of organoclay in an immiscible poly(ethylene terephthalate) waste/ poly(methyl methacrylate) blend," *Journal of Applied Polymer Science*, vol. 117, pp.129–137, 2010.

[12] N. M. L. Mondadori, R. C. R. Nunes, L. B. Canto, and A. J. Zattera, "Composites of recycled PET reinforced with short glass fiber," *Thermoplastic Composite Materials*, vol. 25, pp. 747–764, 2011.

[13] Y. Srithep, A. Javadi, S. Pilla, L. S. Turng, S. Gong, C. Clemons, and J. Peng, "Processing and characterization of recycled poly(ethylene terephthalate) blends with chain extenders, thermoplastic elastomer, and/or poly(butylene adipate-co-terephthalate)," *Polymer Engineering and Science*, vol. 51, pp. 1023–1032, 2011.

[14] M. T. M. Bizarria, A. L. F. M. Giraldi, C. M. Carvalho, J. I. Velasco, M. A. d'Avia, and L.

H. I. Mei, "Morphology and thermomechanical properties of recycled PET-organoclay nanocomposites," *Journal of Applied Polymer Science*, vol. 104, pp. 1839–1844, 2007.

[15] K. P. Chaudhari and D. D. Kale, "Impact modification of waste PET by polyolefinic elastomer," *Polymer International*, vol. 52, pp. 291–298, 2003.

[16] Y. Zhang, H. Zhang, L. Ni, Q. Zhou, W. Guo, and C. Wu, "Characterization and mechanical properties of recycled poly(ethylene terephthalate) toughened by styrene-ethylene/butylenes-styrene elastomer," *Journal of Polymers and the Environment*, vol. 18, pp. 647–653, 2010.

[17] S. C. Chen, L. H. Zhang, G. Zhang, G. C. Zhang, J. Li, X. M. Zhang, and W. X. Chen, "An investigation and comparison of the blending of LDPE and PP with different intrinsic viscosities of PET," *Polymers*, vol. 10, pp. 1–14, 2018.

[18] O. Saravari, H. Waipunya, and S. Chuayjuljit "Effects of ethylene octene copolymer and ultrafine wollastonite on the properties and morphology of polypropylene-based composites," *Journal of Elastomers & Plastics*, vol. 46, pp. 175–186, 2014.

[19] S. Chuayjuljit, A. Larpkasemsuk, P. Chaiwutthinan, D. Pongkao Kashima, and A. Boonmahitthisud, "Effects of analcime zeolite synthesized from local pottery stone as nucleating agent on crystallization behaviors and mechanical properties of isotactic polypropylene," *Journal of Vinyl & Additive Technology*, vol. 24, pp. E85–E95, 2015.

[20] C. P. Papadopoulou and N. K. Kalfoglou, "Comparison of compatibilizer effectiveness for PET/PP blends: their mechanical, thermal and morphology characteristic," *Polymer*, vol 41, pp. 2543-2555, 2000.

[21] A. S. Luyt, M. D. Dramicanin, Z. Antic, and V. Djokovic, "Morphology, mechanical and thermal properties of composites of polypropylene and nanostructures wollastonite filler," *Polymer Testing*, vol. 28, pp. 348–356, 2009.

[22] www.ima-europe.eu./fileadmin/downloads/minerals/wollastonite. November 2010.

[23] S. Chongprakobkit, M. Opaprakasit, and S. Chuayjuljit, "Use of PP-g-MA prepared by solution process as compatibilizer in polypropylene/polyamide 6 blends," *Journal of Metals, Materials and Minerals*, vol. 17, pp. 9–16, 2007.

[24] Y. Lei, Q. Wu, and Q. Zhang, "Morphology and properties of microfibrillar composites based on recycled poly (ethylene terephthalate) and high density polyethylene," *Composites Part A: Applied Science and Manufacturing*, vol. 40, pp. 904–912, 2009.

[25] R. S. Chen, M. H. Ghani, M. N. Salleh, S. Ahmad, and S. Gan, "Influence of blend composition and compatibilizer on mechanical and morphological properties of recycled HDPE/PET blends," *Materials Sciences and Applications*, vol. 5, pp. 943–952, 2014.

[26] Y. Zhang, C. Yu, P. K. Chu, F. Lv, C. Zhang, J. Ji, R. Zhang, and H. Wang, "Mechanical and thermal properties of basalt fiber reinforced poly(butylene succinate) composites," *Materials Chemistry and Physics*, vol. 1338, pp. 845–849, 2012.